3D reservoir characterization of a North Sea oil field using quantitative seismic & CSEM interpretation

Jan Petter Morten[*] and Friedrich Roth, EMGS, David Timko and Constantin Pacurar, Fugro-Jason, Anh Kiet Nguyen and Per Atle Olsen, Statoil

Summary

We have performed a quantitative, joint interpretation of 3D seismic and 3D CSEM data from the Troll Western Oil Province. The presented methodology results in 3D distributions of effective porosity and hydrocarbon saturation. The estimated reservoir property distributions correlate with expected production effects, and we show how hydrocarbon volumes can be assessed.

Introduction

The marine controlled source electromagnetic (CSEM) method for hydrocarbon exploration was introduced ten years ago (Constable, 2010) and is now an established exploration tool. The majority of the CSEM surveys acquired so far have focused on prospect ranking and de-risking (Hesthammer et al., 2010). Traditionally, the survey geometry for these purposes has been a single or a few 2D lines due to limitations in acquisition and processing efficiency. Such datasets may qualitatively differentiate between a low resistivity brine saturated reservoir, and a high resistivity hydrocarbon saturated reservoir. However, interpretations based on 2D are only reliable in cases where 3D effects can be ignored, and when the reservoir outline is known with high confidence so that the towline can be positioned optimally.

The application window has since the introduction of the method been expanded to include frontier exploration, where large-scale, coarse 3D grid surveys can be a very useful tool (Suffert et al., 2008; Morten et al., 2009). In these situations, it is essential to go to 3D acquisition with azimuth data as demonstrated in Morten et al. (2009). The target geometry estimated without azimuth data could be inaccurate, so that a dataset consisting of 2D lines gives too little information for a reliable interpretation. Moreover, the lateral mapping provided by 3D acquisition can indicate new leads not previously identified in e.g. seismic interpretation.

CSEM applications relevant for the later stages of petroleum operations have been addressed in quantitative reservoir characterization studies on real data (see e.g. Hoversten et al., 2006; Harris et al., 2009; Dell'Aversana et al., 2011), and in feasibility studies for CSEM monitoring (Orange 2009; Zach 2009). These studies have demonstrated that the technique can be used not only to differentiate qualitatively between brine and hydrocarbon saturation, but also to quantitatively predict fluid distributions and even reservoir properties by integration with seismic and well data. So far the published real data applications use 2D data only and have focused on vertical profiles. For resource estimation and field appraisal, the lateral perimeter of the hydrocarbon saturated reservoir zone that can be mapped with 3D CSEM is essential. In this abstract, we demonstrate using real data from the Troll Western Oil Province (TWOP, see Figure 1) how quantitative, joint interpretation of CSEM, seismic, and well data can yield 3D fluid distribution models to study production effects and give hydrocarbon volume estimates.

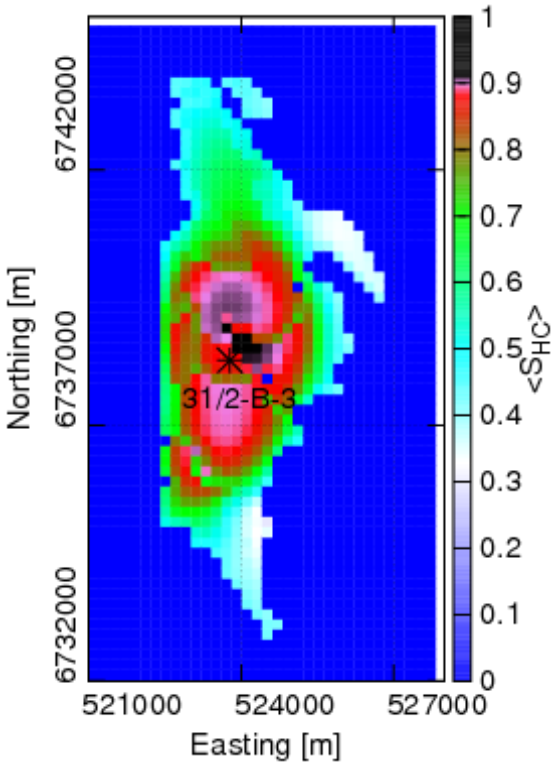

Figure 1: Troll Western Oil Province hydrocarbon saturation averaged over the total pore column. The central part close to the indicated gas injection well 31/2-B-3 (*) is mapped with anomalously high saturation.

We will first describe the methodology applied to obtain 3D distributions for porosity and hydrocarbon saturation.

Then, we discuss some of the prominent features apparent in the results, and correlate to expected production effects. Finally, we demonstrate by a modeling example that for the TWOP studied here, 3D effects substantially influence the CSEM data thereby making reservoir characterization from 2D acquisition and data processing questionable.

Field data

The Troll field is the biggest gas field in the North Sea, and has been producing since 1996 (Mikkelsen et al., 2005). Significant quantities of oil are also present as thin zones under the gas cap. In this study, we focus on the TWOP (see Figure 1), which is a smaller (25 km^2) segment of the reservoir where the oil column before production was thicker (15-27 m oil, 8-43 m gas). The oil is produced from horizontal wells placed close to the oil water contact, with pressure support by gas injection. TWOP is situated in a rotated fault block tilted toward east. The sediments consist of alternating layers of clean medium to coarse grained high permeability sand, and micaceous fine grained sands and siltstone with low to medium permeability, deposited in a shallow marine environment influenced by tidal and fluvial processes.

An extensive geophysical database is available for TWOP, but to simulate an appraisal phase of the development, we have used only logs from the exploration wells that were drilled 1984-1985. Repeated 3D seismic is acquired; we have used data from the 2003 acquisition. Additionally, we used CSEM data from an R&D 3D CSEM survey acquired in 2008 in collaboration between Statoil and EMGS (Gabrielsen et al., 2009). The survey included 54 receivers with 1.25 km spacing, and 9 towlines oriented in two orthogonal directions.

Petrophysics

The publicly available exploration well logs underwent extensive data QC and conditioning. Some logs were not available for any or the whole logged interval; in particular the shear sonic log was lacking. The petrophysical analysis established rock physics models for seismic and electric properties. For the reservoir interval, we obtained a consistent interpretation of the effective water saturation and the effective porosity, which excludes bound water. Effects from calcite and clay inclusions in the reservoir were considered, and are not expected to give large contributions to the seismic and CSEM data.

Our analysis of the well data shows that there are strong correlations between effective porosity and P-impedance, and between resistivity and water saturation. This is consistent with the findings in Hoversten et al. (2006). Thus, separate 3D impedance and resistivity distributions can establish both the pore volume and fluid content. Such information can be obtained from inversion of the seismic and CSEM data. Further analysis of the well data shows that resistivity and P-impedance are weakly correlated. Therefore, we may perform uncoupled inversions on seismic and CSEM data since the two geophysical data are controlled by independent reservoir parameters.

Mapping inversion results to reservoir properties

The conditioned well logs and seismic horizons were used to estimate the wavelet and then create a low-frequency model for the seismic inversion. Using publicly available post-stack migrated seismic data, we carried out full stack inversion. This resulted in a P-impedance model with good well tie. Cross-plotting P-impedance to effective porosity using upscaled well data from the reservoir zone reveals good correlation so that a trend curve can be constructed. Using this trend curve, the 3D P-impedance distribution is transformed into an effective porosity distribution for the reservoir.

An initial model for the anisotropic 3D CSEM inversion was created from profiles resulting from 1D inversion based on a simulated annealing algorithm. A structural constraint for the hydrocarbon zone of the reservoir is determined by the seismic top reservoir horizon and the oil-water contact depth observed in the exploration wells. Using this information, regularization was formulated to favor typical formation resistivity in the background, and allowing anomalously large resistivity associated with hydrocarbons inside the hydrocarbon saturated part of the reservoir. The resistivity model produced by 3D inversion thus incorporates the resistive body due to the TWOP with structure as defined from the top reservoir horizon and oil water contact. The final 3D inversion model generally has data misfit to the observed data which is of the order of the data uncertainty.

In order to go from the vertical resistivity reconstructed inside the hydrocarbon zone of the reservoir to water saturation, a trend curve based on well data was established. To reflect information at the same scale as the CSEM data, the measured well resistivity logs were first upscaled to agree with CSEM resolution, resulting in a vertical and a horizontal resistivity. The well log derived vertical resistivity is then cross-plotted to the water saturation averaged over the pore volume of the depth intervals used for the resistivity log upscaling. The cross-plot reveals a strong trend to which a Simandoux rock physics model is fitted. This model is then used to transform the 3D inversion model for vertical resistivity into a water saturation distribution.

Analysis

The 3D distributions for effective porosity and water saturation (see Figure 1) obtained from inversion can be used for various reservoir characterization studies. For example, information about reservoir quality can be inferred from the mapped porosity variations, and the perimeter of the hydrocarbon saturated zone can be inferred from the water saturation distribution. Production effects can be studied by correlating anomalies in the water saturation in high permeability regions to the expected changes in fluid distribution. Hydrocarbon volume estimates can be calculated by combining information about porosity φ and saturation S_{HC} as shown in the hydrocarbon pore column map in Figure 2. This map shows the lateral hydrocarbon distribution calculated as the vertical integral of hydrocarbon pore volume at each lateral position, $\sum_z S_{HC}\,\varphi\,\Delta z$. The map is thus strongly correlated to reservoir thickness; a thicker hydrocarbon column gives a larger contribution to the integral. Computing the integral also over the lateral extent of the reservoir gives the total hydrocarbon volume. This volume can be directly compared to data from the operator's reservoir model, which is the aim of an ongoing collaboration with the Troll license group.

Contributions to the lateral variation in the hydrocarbon pore column not related to reservoir thickness variations are more clearly visualized in Figure 1. In this map, we show the hydrocarbon saturation averaged over the total pore column, $\sum_z S_{HC}\,\varphi\,\Delta z \Big/ \left(\sum_z \varphi\,\Delta z\right)$. An anomalously large saturation can be observed close to the indicated position of the gas injection well which provides production pressure support. At the time of the CSEM acquisition, gas injection had been ongoing for 12 years, so local effects on the fluid distribution and saturation can be expected. The exploration well logs analyzed in this work show that typically, the gas zone is associated with lower water saturation and hence larger resistivity than the oil zone. Therefore, an expanded gas cap with a possible local increase in hydrocarbon saturation or volume resulting from the gas injection may be the cause of the observed anomaly in the estimated saturation. The extent of the region with very large hydrocarbon or injected gas saturation seen in Figure 1 seems limited southwards by a known fault with a North-West strike direction.

2D versus 3D quantitative CSEM interpretation

The information about lateral variations and the hydrocarbon volume estimation discussed above can only be obtained from 3D acquisition and processing. To assess the feasibility of quantitative interpretation in terms of 2D sections from 2D acquisition and anisotropic 2.5D inversion, we have performed a CSEM modeling study. One of the North-South oriented towlines in the 3D grid was situated approximately 1 km from the western edge of the reservoir, see Figure 2. We will use data from 7 inline receivers on this towline to study the magnitude of 3D effects in the data (survey details: Gabrielsen et al., 2009).

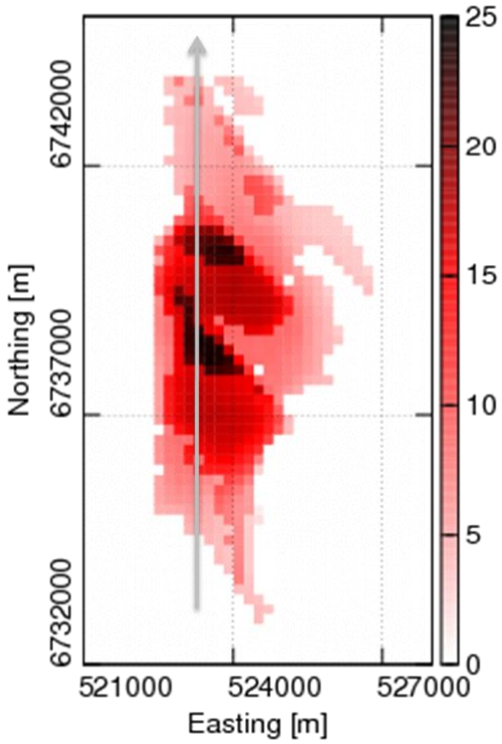

Figure 2: Estimated hydrocarbon pore column. The map is strongly correlated to reservoir thickness, with additional structures due to 3D porosity and saturation variations. They grey arrow indicates the approximate position of the towline used to assess 2.5D modeling accuracy (see text).

Since the 3D inversion resistivity model reproduces the observed data to within the measurement accuracy (Figure 3), we assume that this model can be used as a reference for the resistivity anomaly associated with TWOP. We created a 2D model from the obtained 3D inversion result by extracting a 2D resistivity section along the indicated towline. This section is used for 2.5D modeling, which assumes that the resistivity distribution is invariant transverse to the towline, but simulates the 3D variation of the electromagnetic fields within such a model. The finite extent and lateral variation of the TWOP perpendicular to

the towline not accounted for in the 2.5D modeling will introduce modeling errors which we seek to estimate.

Figure 3 shows the misfit between synthetic and observed data computed as $\left|E_{synthetic} - E_{observed}\right| / \left|E_{observed}\right|$ for the discussed towline. The top plot shows the misfit from 3D modeling of the 3D resistivity model. The misfit is below 0.1, and typically lower than measurement uncertainty. The bottom plot shows the misfit when 2.5D modeling is applied for the 2D model. The data which are mainly affected by the background resistivity exhibit low misfit comparable to 3D modeling. However, the data points in the plot where significant influence from the TWOP is expected, have large misfit. We believe this is due to 3D effects, which for the given survey layout and reservoir geometry strongly influence the data so that the 2D assumption is violated. This indicates that reservoir characterization in terms of 2D resistivity sections obtained from anisotropic 2.5D inversion will be inaccurate. Specifically, the 3D effects demonstrated by this modeling study would lead to an underestimation of the reservoir resistivity by 2.5D inversion. Following the interpretation methodology described here, this would result in a systematic error giving too low hydrocarbon saturation.

Conclusions

In this abstract, we have shown how 3D distributions of reservoir parameters can be obtained in a joint, quantitative interpretation of 3D seismic and 3D CSEM data. We emphasize the importance of 3D CSEM acquisition in combination with anisotropic 3D inversion, which enables us to study lateral variations of the hydrocarbon saturation, and calculate hydrocarbon volume estimates. A modeling example for one of the survey lines shows that the data are strongly affected by 3D effects, so that reservoir characterization relying on a 2D assumption is likely to give inaccurate results.

Validation of the results presented here for the Troll Western Oil Province is ongoing in collaboration with the Troll license group. An extensive database is available for the field, and direct comparison to results incorporating information from an extensive well log database will address the accuracy of the predictions. Encouraged by the preliminary results, we look ahead regarding the potential use of the methodology. The input dataset is representative of what would be available in an appraisal setting, for which these results could be of great utility in delineation and planning of further appraisal wells. There is also potential for development planning with fewer wells, as well as for reserve estimation. Large-scale production effects may also be inferred, which is the aim of monitoring for drainage/injection effects and optimizing production.

Acknowledgments

We acknowledge the Troll partners Statoil, Petoro, Shell, ConocoPhillips, and Total for their input to the ongoing validation of the reservoir characterization results.

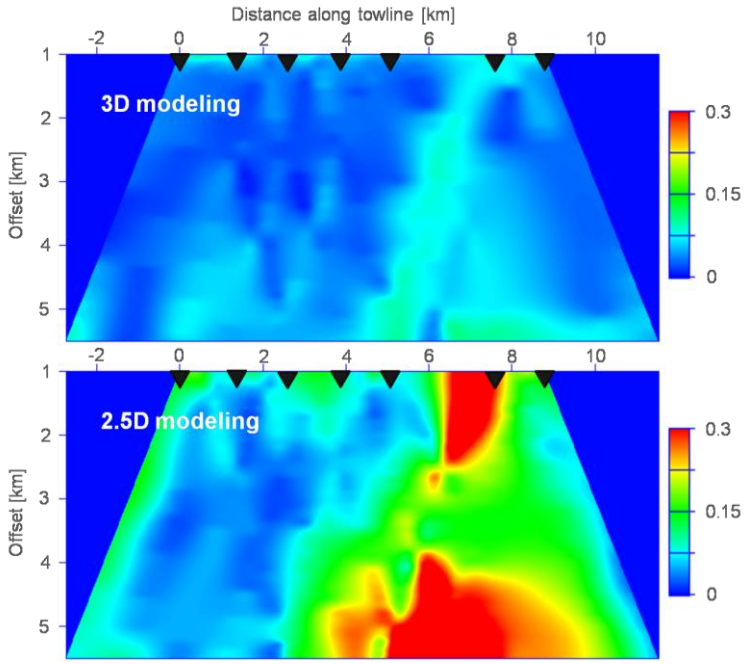

Figure 3: Misfit between synthetic (top: 3D modeling, bottom: 2.5D modeling) and observed data for inline electric field at 0.75 Hz. The misfit is displayed at CMP positions, with interpolation between data points. The towline position is indicated in Figure 2. The large misfit area at long offset in the 2.5D case is due to data points associated in CMP with the thickest part of TWOP.

EDITED REFERENCES

Note: This reference list is a copy-edited version of the reference list submitted by the author. Reference lists for the 2011 SEG Technical Program Expanded Abstracts have been copy edited so that references provided with the online metadata for each paper will achieve a high degree of linking to cited sources that appear on the Web.

REFERENCES

Constable, S., 2010, Ten years of marine CSEM for hydrocarbon exploration: Geophysics, **75**, no. 5, 75A67–75A81, doi:10.1190/1.3483451.

Dell'Aversana, P., S. Carbonara, S. Vitale, M. A. Subhani, and J. Otiocha, 2011, Quantitative estimation of oil saturation from marine CSEM data: A case history: First Break, **29**, 53.

Harris, P. E., Z. Du, L. MacGregor, W. Olsen, R. Shu, and R. Cooper, 2009, Joint interpretation of seismic and CSEM data using well log constraints: an example from the Luva Field: First Break, **27**, 73.

Hesthammer, J., A. Stefatos, M. Boulaenko, S. Fanavoll, and J. Danielsen, 2010, CSEM performance in light of well results: The Leading Edge, **29**, 34, doi:10.1190/1.3284051.

Hoversten, G. M., F. Cassassuce, E. Gasperikova, G. A. Newman, J. Chen, Y. Rubin, Z. Hou, and D. Vasco, 2006, Direct reservoir parameter estimation using joint inversion of marine seismic AVA and CSEM data: Geophysics, **71**, no. 3, C1–C13.

Gabrielsen, P. T., I. Brevik, R. Mittet, and L. O. Løseth, 2009, Investigating the exploration potential for 3D CSEM using a calibration survey over the Troll Field: First Break, **27**, 67.

Mikkelsen, J. K., T. Norheim, and S. I. Sagatun, 2005, The troll story: OTC 17108.

Morten, J. P., A. K. Bjørke, T. Støren, E. Coward, S. A. Karlsen, and F. Roth, 2009a, Importance of azimuth data for 3D inversion of marine CSEM scanning data: 71st Annual International Conference and Exhibition, EAGE, Extended Abstracts, X005.

Orange, A., K. Key, and S. Constable, 2009, The feasibility of reservoir monitoring using time-lapse marine CSEM: Geophysics, **74**, no. 2, F21–F29, doi:10.1190/1.3059600.

Suffert, J., P. Sangvai, F. Roth, A. Tyagi, and R. Bastia, 2008, Frontier exploration by electromagnetic scanning — A deep water example: 79th Annual International Meeting, SEG, Expanded Abstracts, **27**, 662–666, doi:10.1190/1.3063737.

Zach, J. J., M. A. Frenkel, D. Ridyard, J. Hincapie, B. Dubois, and J. P. Morten, 2009, Marine CSEM time-lapse repeatability for hydrocarbon field monitoring: 79th Annual International Meeting, SEG, Expanded Abstracts, **28**, 820–824, doi:10.1190/1.3255878.